Available online at www.sciencedirect.com
ScienceDirect
Journal of Nuclear Materials 363–365 (2007) 972–976
journal of nuclear materials
www.elsevier.com/locate/jnucmat

Properties of hydrogen desorption from co-deposits on JT-60 graphite tile by pulsed-laser ablation

D. Watanabe [a,*], Y. Sakawa [b], T. Shibahara [a], K. Sugiyama [c], T. Shoji [a], K. Yamazaki [a], T. Tanabe [c]

[a] *Nagoya University, Chikusa-ku, Nagoya 464-8603, Japan*
[b] *Institute of Laser Engineering, Osaka University, Yamadaoka, Suita 565-0871, Japan*
[c] *Interdisciplinary School of Engineering, Kyusyu University, Fukuoka 812-8581, Japan*

Abstract

For the purpose of tritium removal from carbon co-deposits on plasma-facing material of fusion device, pulsed-laser induced desorption of hydrogen from co-deposits on JT-60 open-divertor tile has been investigated. The fundamental (1064 nm) and fourth harmonic (266 nm) emission of a 20 ps-Nd: YAG laser were used, and dependences of hydrogen desorption on laser intensity I_L and wavelength λ were studied. Hydrogen-desorption efficiency, defined as the ratio between the number of desorbed hydrogen by laser irradiation and that of hydrogen retained in the ablated volume, was largest in the region, where strong ionization of C^+ occurred, and was larger for $\lambda = 266$ nm, in which a laser photon can cut C–H bond, compared with that for $\lambda = 1064$ nm. For the ablative removal of hydrogen, a short-wavelength and high-power laser is desirable.

PACS: 28.52.−s; 78.20.Ci; 79.20.Ds; 79.20.La

Keywords: Ablation; Carbon-based material; Desorption; Laser; Tritium

1. Introduction

Carbon materials are one of the candidates for plasma-facing materials in ITER and nuclear-fusion reactors because of its superior nature at high-heat flux and low-atomic number. However, when carbon is eroded by hydrogenic plasmas containing tritium, it co-deposits with tritium, and periodical removal is required from the safety reason [1]. Glow-discharge cleaning (GDC) is used or planned in many tokamaks including ITER [1], although hydrogen isotopes retained in the shadow area of the glow-discharge plasma are hardly removed. Laser-induced desorption (LID) is proposed as one of the tritium removal methods and has advantages of practicability even for the shadow area through optics and robotics [2]. Therefore LID is suitable for utilization together with GDC.

We have studied laser-ablation properties of a hydrogen-saturated graphite target, 10 keV

* Corresponding author. Fax: +81 52 789 3938.
E-mail address: d-watanabe@ees.nagoya-u.ac.jp (D. Watanabe).

0022-3115/$ - see front matter © 2007 Elsevier B.V. All rights reserved.
doi:10.1016/j.jnucmat.2007.01.134

hydrogen- or 8 keV deuterium-implanted graphite targets, using a pulsed eximer laser (193 nm) [3,4] and the fourth harmonic (266 nm) emission of a 20 ps-Nd: YAG laser [4,5]. A pulsed-laser irradiation of co-deposits on JT-60 open-divertor tile has also been investigated using the 266 nm-laser, and the dependences of laser-ablation and hydrogen-desorption properties on laser intensity I_L have been studied [6].

In this paper, LID of hydrogen-retained co-deposits on JT-60 open-divertor tile has been investigated using the fundamental ($\lambda = 1064$ nm) and fourth harmonic ($\lambda = 266$ nm) emission of a 20 ps-Nd: YAG laser over a wide region of I_L, and dependences of hydrogen desorption on I_L and λ have been studied.

2. Experimental procedure

Experiments were conducted under the vacuum pressure $<3\times10^{-8}$ Torr. The fundamental ($\lambda = 1064$ nm) and fourth harmonic ($\lambda = 266$ nm) emission of Nd: YAG laser (Continuum Custom PY61C-10, laser energy <35 mJ/pulse for 1064 nm and <3 mJ/pulse for 266 nm, pulse duration ~20 ps, $I_L < 6\times10^{12}$ W/cm^2 for 1064 nm and 5×10^{11} W/cm^2 for 266 nm, repetition rate = 10 Hz) were used. Laser beam was introduced to the target surface through a quartz window with a normal direction using a quartz lens with a focal length of 300 mm. I_L was varied mainly by changing the focal-spot size, and 1000 shots of the laser pulses were irradiated on the target. Emitted ions were measured by a time-of-flight mass spectrometer (TOFMS), and visible-light emission was monitored by a spectrometer (Hamamatsu C7473); both measurements were conducted at 45° from the laser pass. Desorbed gases were measured by a quadrupole mass spectrometer (QMS: ULVAC MSQ-150), and we measured both mass spectra (scan range is $m/e = 1$–80, scan speed is ~0.5 s/scan) and time evolution of H_2 gas until 50 s with a fixed m/e of 2. QMS was calibrated to give a partial pressure of H_2 gas using a calibrated ionization vacuum gauge. Laser-spot size and ablation depth were measured by scanning electron microscopy (SEM) and an optical microscope, respectively.

One of the JT-60 open-divertor tiles was used as a sample. The tile was exposed to 1800 hydrogen discharges from June 1988 to October 1988 with the limiter configuration including 300 lower X-point divertor configurations. The sample was cut from the inner-divertor area with a dimension of about $30\times10\times1$ mm^3. We observed a cross-sectional view of the sample by SEM and found that the co-deposits completely covered the tile with the thickness of about 35–55 μm. The thickness was in good agreement with that reported by Gotoh et al. [7].

3. Results

Fig. 1(a) shows ablation depth per laser shot (Δd) versus I_L. A logarithmic dependence of Δd on I_L is known as Beer's law, $\Delta d = \alpha^{-1}\ln(I_L/I_{ablation})$, where α is the linear absorption-coefficient and $I_{ablation}$ is the threshold laser intensity for ablation [8,9]. Error bars represent the sum of the surface roughness of the co-deposits and statistical error. Fitting of Δd against I_L using Beer's law gives $I_{ablation} = 9.0\times10^9$ W/cm^2 and $\alpha = 35$ μm^{-1} for $\lambda = 266$ nm, and $I_{ablation} \sim 1.0\times10^{10}$ W/cm^2 and $\alpha \sim 15$ μm^{-1} for $\lambda = 1064$ nm. Shu et al. have reported that the measured value of α for JT-60 co-deposits using a 25 ns-193 nm laser was 1.9 μm^{-1} [8]. The reason for the discrepancy in α is probably due to the difference in the pulse duration and wavelength of the laser.

Δd against I_L for $\lambda = 1064$ nm up to $I_L \sim 6\times10^{12}$ W/cm^2 is re-plotted in Fig. 1(b). Since the maximum depth that we could measure using the optical microscope was ~300 μm, we could not determine Δd at $I_L > 4.0\times10^{11}$ W/cm^2. However, at $I_L > 1.0\times10^{12}$ W/cm^2, the penetration holes were

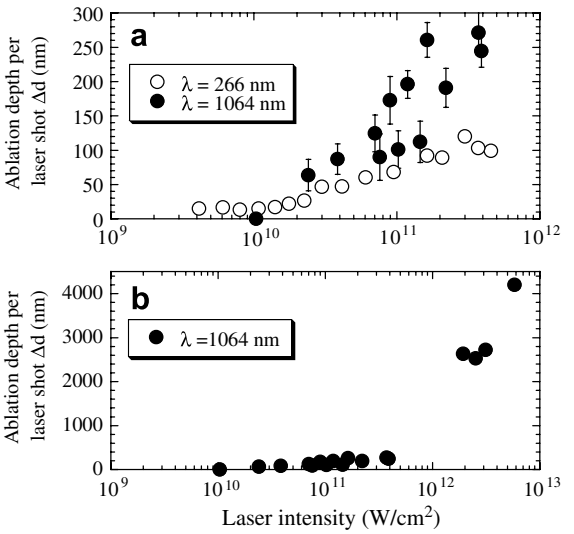

Fig. 1. Ablation depth per laser shot Δd versus laser intensity I_L for (a) $\lambda = 266$ [6] and 1064 nm up to $I_L \sim 5\times10^{11}$ W/cm^2 and (b) for $\lambda = 1064$ nm up to $I_L \sim 6\times10^{12}$ W/cm^2.

observed on the sample of 1 mm in thickness after the laser irradiation of 1000 shots. Therefore, we have determined Δd from the time evolution of H_2 signal intensity ($I[H_2]$) in QMS; $I[H_2]$ drastically increased when the ablation depth reached 1 mm and the sample holder was irradiated by the laser. Δd for $\lambda = 1064$ nm was enhanced at $I_L > (3.4–7.4) \times 10^{11}$ W/cm^2 and was expressed by two logarithmic curves.

For $\lambda = 266$ nm, we have distinguished three I_L regions, non-ablation region (NAR_{266}: $I_L < 9.0 \times 10^9$ W/cm^2), weak-ablation region (WAR_{266}: 9.0×10^9 W/cm$^2 < I_L < 9.0 \times 10^{10}$ W/cm^2) and strong-ablation region (SAR_{266}: $I_L > 9.0 \times 10^{10}$ W/cm^2) [6]. In SAR_{266}, strong-ionization of carbon occurred. WAR_{266} is the region where above and below the threshold laser intensities of ablation and the strong-ionization of carbon, respectively [6].

In the TOFMS measurements for $\lambda = 1064$ nm, C^+ ($I[C^+]$) and C_n^+ ($I[C_n^+]$) signal intensities were dominant at I_L larger and less than $(3.4–7.4) \times 10^{11}$ W/cm^2, respectively. This I_L corresponds to $I_{ionization}$, and we could distinguish three I_L regions, similar to the $\lambda = 266$ nm case; NAR_{1064} at $I_L < 1.0 \times 10^{10}$ W/cm^2, WAR_{1064} at 1.0×10^{10} W/cm$^2 < I_L < (3.4–7.4) \times 10^{11}$ W/cm^2, and SAR_{1064} at $I_L > (3.4–7.4) \times 10^{11}$ W/cm^2. Thus, $I_{ionization} = (3.4–7.4) \times 10^{11}$ W/cm^2 for $\lambda = 1064$ nm was by a factor of 4–8 larger than $I_{ionization} = 9.0 \times 10^{10}$ W/cm^2 for $\lambda = 266$ nm. Amoruso et al. have reported that $I_{ionization}$ was determined by the threshold I_L for multi-photon ionization (MPI) and inverse bremsstrahlung (IB) absorption [10]. Since the ionization energy of carbon is 11.26 eV, three-photon ionization can occur for the 266 nm-laser (4.66 eV), while photon energy is much lower for the 1064 nm-laser (1.17 eV). The larger value of $I_{ionization}$ for $\lambda =$ 1064 nm is probably caused by the less effective MPI.

Fig. 2(a) shows time evolution of H_2 desorption rate, which is determined by $I[H_2]$ and the measured pumping speed, and divided by a laser-spot size. Succeeding stepwise increases in $I[H_2]$ at every 0.1 s correspond to the desorption of H_2 gas by each laser shot. The difference in noise levels was caused by the different sensitivities in QMS measurement. H_2 desorption rate for $\lambda = 1064$ nm decreased more than an order of magnitude and became almost noise level in few seconds; much faster than that for $\lambda = 266$ nm. This tendency is caused by the difference in the amount of the desorbed H_2 molecules per laser shot ($\Delta I[H_2]$), which is calculated by the

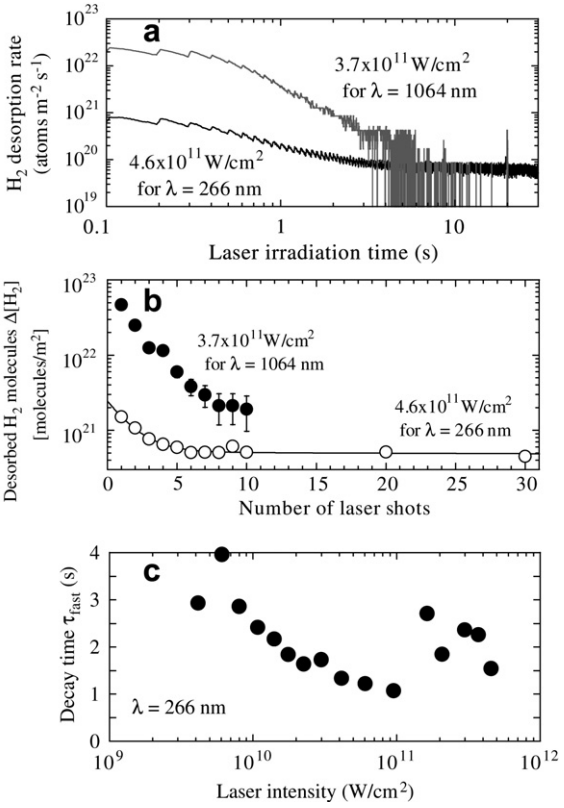

Fig. 2. (a) H_2 desorption rate per ablation-spot size versus laser-irradiation time and (b) the amount of desorbed H_2 molecules per laser shot $\Delta I[H_2]$ derived from (a) versus the number of the laser shot at $I_L = 3.7 \times 10^{11}$ W/cm^2 for $\lambda = 1064$ nm and $I_L = 4.6 \times 10^{11}$ W/cm^2 for $\lambda = 266$ nm [6]. (c) Decay time τ_{fast} for $\lambda = 266$ nm versus laser intensity.

amount of increment in $I[H_2]$ per laser pulse (Fig. 2(b)). $\Delta I[H_2]$ was largest at the first laser shot and decreased with time both for $\lambda = 266$ and 1064 nm. $\Delta I[H_2]$ in NAR_{1064} and WAR_{1064} became noise level within ~20 shot. It seemed that the decrease in $\Delta I[H_2]$ were superposed by two processes, a fast-desorption process (FDP) and a slow-desorption process (SDP) for $\lambda = 266$ nm. FDP and SDP were approximated by exponential-decay curves, that is $\Delta I[H_2] = \Delta I[H_2]_{fast}\exp(-t/\tau_{fast}) + \Delta I[H_2]_{slow}\exp(-t/\tau_{slow})$. Here, $\Delta I[H_2]_{fast}$ ($\Delta I[H_2]_{slow}$) and τ_{fast} (τ_{slow}) are $\Delta I[H_2]$ at $t = 0$ and decay time for FDP (SDP), respectively, and t is the time from the beginning of the laser irradiation. Measured τ_{fast} for $\lambda = 266$ nm is shown in Fig. 2(c); it decreased by increasing I_L in WAR_{266} and increased by a factor of 2–3 in SAR_{266}, while, τ_{slow} was nearly constant on I_L (not shown).

Fig. 3 represents the ratio between the number of the desorbed H_2 molecules ($N_{desorbed}$) and that

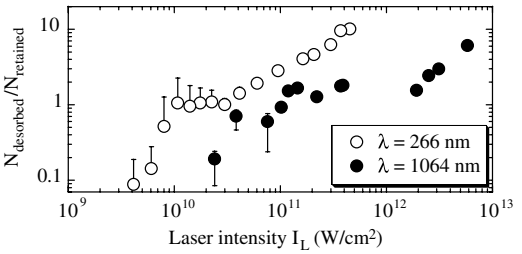

Fig. 3. The ratio between the number of desorbed H_2 molecules ($N_{desorbed}$) and that of hydrogen retained in the ablated volume ($N_{retained}$) [6]. $N_{desorbed}$ was obtained by integrating H_2 desorption rate from the beginning of the laser irradiation until t_1. Here, t_1 is 30 s for $\lambda = 266$ nm and is the time when ablation depth reaches the thickness of the co-deposits for $\lambda = 1064$ nm.

retained in the ablated volume ($N_{retained}$) against I_L; $N_{desorbed}/N_{retained}$ or hydrogen-removal efficiency vs I_L. $N_{desorbed}$ was obtained by integrating H_2 desorption rate shown in Fig. 2(a) from the beginning of the laser irradiation until t_1, which was 30 s for $\lambda = 266$ nm and was the time when the ablation depth reached the thickness of co-deposits (maximum t_1 was fixed as 30 s) for $\lambda = 1064$ nm. $N_{retained}$ was calculated from the density of hydrogen in the co-deposits and the ablation volume; the ablation depth by laser irradiation until t_1 and laser-spot size assuming a parabolic radial ablation profile. Hydrogen was retained homogeneously in the co-deposits with nearly constant concentration of $H/C = 0.03$ or 1.4×10^{21} atoms m^{-2} μm^{-1} [11]. Error bars appeared from the errors in Δd shown in Fig. 1(a) and 1(b). $N_{desorbed}/N_{retained}$ for $\lambda = 266$ nm was below 1 in NAR_{266}, nearly equal to 1 in WAR_{266}, and over 3 in SAR_{266} [6]. For $\lambda = 1064$ nm, $N_{desorbed}/N_{retained}$ increased with I_L and was larger than 1 at $I_L > 10^{11}$ W/cm^2. A possible reason why the $N_{desorbed}/N_{retained}$ values exceeded 1 is the thermal desorption from the region surrounding the ablated volume owing to temperature increase caused by the succeeding laser irradiation. Temperature of the ablated volume and that of the surrounding region are above and below 3800 °C, which is sublimation temperature of carbon. Since we calculated the number of desorbed hydrogen only as H_2 molecules, if we include that as hydrocarbon molecules, $N_{desorbed}/N_{retained}$ becomes larger.

4. Discussion

Fig. 1(a) and (b) indicates that ablative-removal rate of co-deposits for $\lambda = 1064$ nm is larger than that for $\lambda = 266$ nm. However, since the ablated carbon clusters containing tritium may re-deposit near the laser spot, it is also required to remove tritium from ablated co-deposits. Therefore, it is better to remove tritium as gas. Hydrogen-removal efficiency ($N_{desorbed}/N_{retained}$) for $\lambda = 266$ nm was larger than that for $\lambda = 1064$ nm, and the 266 nm-laser is more suitable for tritium removal from fusion device than the 1064-nm laser. A possible reason for the observed difference in $N_{desorbed}/N_{retained}$ for $\lambda = 266$ and 1064 nm is the following: Since the photon energies of $\lambda = 266$ and 1064 nm are 4.66 and 1.17 eV, respectively, only 266 nm-photons can cut C–H bond with bonding energy of 4.5 eV.

We also investigated that the ratio between the number of C_2H_2 and H_2 molecules desorbed during 300 shots of the 266-nm laser irradiation increased with I_L in NAR_{266} and WAR_{266}, while, it decreased with I_L in SAR_{266} [6]. Since most of hydrocarbons have large sticking coefficients, they can be easily deposited on the line of sight surface of vacuum vessel. Therefore, SAR_{266} is suitable since larger amount of the accumulated tritium is removed efficiently as tritium gas [6].

5. Summary

Co-deposits on JT-60 open-divertor tile were irradiated by the fundamental (1064 nm) and fourth harmonic (266 nm) emission of a 20 ps-Nd: YAG laser, and dependencies of properties of ablation and hydrogen desorption on I_L and λ were investigated. Ablation depth per laser shot Δd versus I_L showed that whereas $I_{ablation} \sim 10^{10}$ W/cm^2 was nearly independent on λ the linear absorption-coefficient α was larger for $\lambda = 266$ nm ($\alpha = 35$ and 15 μm^{-1} for $\lambda = 266$ and 1064 nm, respectively). A large difference in $I_{ionization}$ between $\lambda = 1064$ and 266 nm was observed; $I_{ionization} = 9 \times 10^{10}$ and $(3.4–7.4) \times 10^{11}$ W/cm^2 for $\lambda = 266$ and 1064 nm, respectively. The lower $I_{ionization}$ for $\lambda = 266$ nm was explained by three-photon ionization of carbon. The amount of the desorbed H_2 molecules per laser shot $\Delta I[H_2]$ was largest at the first laser shot. $\Delta I[H_2]$ became almost noise level within ~20 shots of laser irradiation for $\lambda = 1064$ nm and decreased with I_L as a sum of two exponential-decay curves for $\lambda = 266$ nm. Hydrogen-removal efficiency $N_{desorbed}/N_{retained}$ was largest in SAR and was larger for $\lambda = 266$ nm than for $\lambda = 1064$ nm. SAR with a short-wavelength laser is more desirable for removal of hydrogen isotopes.

Acknowledgements

This work has been partly supported by a Grant-in-Aid for Scientific Research by the Ministry of Education, Culture, Sports, Science and Technology of Japan (Grant Nos. 17540468 and 17206092).

References

[1] G. Federici, R.A. Anderl, P. Andrew, J.N. Brooks, R.A. Causey, J.P. Coad, D. Cowgill, R.P. Doemer, A.A. Haasz, G. Janeschitz, W. Jacob, G.R. Longhurst, R. Nygren, A. Peacock, M.A. Pick, V. Philipps, J. Roth, C.H. Skinner, W.R. Wampler, J. Nucl. Mater. 266–269 (1999) 14.

[2] C.H. Skinner, H. Kugel, D. Mueller, B.L. Doyle, W.R. Wampler, in: Proceedings of the 17th IEEE/NPSS Symposium on Fusion Engineering, San Diego, 1997, IEEE Piscataway, NJ, USA, 1998, p. 321.

[3] T. Shibahara, Y. Sakawa, T. Tanabe, J. Nucl. Mater. 337–339 (2005) 654.

[4] Y. Sakawa, T. Shibahara, K. Sato, T. Tanabe, J. Plasma Fusion Res. Series 7 (2006) 138.

[5] Y. Sakawa, K. Sato, T. Shibahara, T. Tanabe, Fusion Eng. Des. 81 (2006) 381.

[6] Y. Sakawa, D. Watanabe, T. Shibahara, K. Sugiyama, T. Tanabe, J. Nucl. Mater., in press.

[7] Y. Gotoh, T. Arai, J. Yagyu, K. Masaki, K. Kodama, N. Miya, J. Nucl. Mater. 329–333 (2004) 840.

[8] W.M. Shu, Y. Kawakubo, K. Masaki, M.F. Nishi, J. Nucl. Mater. 313–316 (2003) 584.

[9] S.R. Cain, F.C. Burns, J. Appl. Phys. 71 (1992) 4107.

[10] A. Amoruso, R. Bruzzese, N. Spinelli, R. Velotta, J. Phys. B, At. Mol. Opt. Phys. 32 (1999) R131.

[11] Y. Hirohata, T. Shibahara, T. Tanabe, T. Arai, Y. Gotoh, Y. Oya, H. Yoshida, Y. Morimoto, J. Yagyu, K. Masaki, K. Okuno, T. Hino, N. Miya, J. Nucl. Mater. 337–339 (2005) 609.